© 2023. Published by The Company of Biologists Ltd | Development (2023) 150, dev201868. doi:10.1242/dev.201868

RESEARCH ARTICLE

Frizzled2 receives WntA signaling during butterfly wing pattern formation

Joseph J. Hanly[1,2,*], Ling S. Loh[1,*], Anyi Mazo-Vargas[1], Teomie S. Rivera-Miranda[3], Luca Livraghi[1,2,4], Amruta Tendolkar[1], Christopher R. Day[1,5], Neringa Liutikaite[1], Emily A. Earls[1], Olaf B. W. H. Corning[1], Natalie D'Souza[1], José J. Hermina-Perez[1], Caroline Mehta[1], Julia A. Ainsworth[6], Matteo Rossi[7], Riccardo Papa[3,8,9], W. Owen McMillan[2], Michael W. Perry[6] and Arnaud Martin[1,2,‡]

ABSTRACT

Butterfly color patterns provide visible and biodiverse phenotypic readouts of the patterning processes. Although the secreted ligand WntA has been shown to instruct the color pattern formation in butterflies, its mode of reception remains elusive. Butterfly genomes encode four homologs of the Frizzled-family of Wnt receptors. Here, we show that CRISPR mosaic knockouts of *frizzled2* (*fz2*) phenocopy the color pattern effects of *WntA* loss of function in multiple nymphalids. Whereas *WntA* mosaic clones result in intermediate patterns of reduced size, *fz2* clones are cell-autonomous, consistent with a morphogen function. Shifts in expression of *WntA* and *fz2* in *WntA* crispant pupae show that they are under positive and negative feedback, respectively. Fz1 is required for Wnt-independent planar cell polarity in the wing epithelium. Fz3 and Fz4 show phenotypes consistent with Wnt competitive-antagonist functions in vein formation (Fz3 and Fz4), wing margin specification (Fz3), and color patterning in the Discalis and Marginal Band Systems (Fz4). Overall, these data show that the WntA/Frizzled2 morphogen-receptor pair forms a signaling axis that instructs butterfly color patterning and shed light on the functional diversity of insect Frizzled receptors.

KEY WORDS: Evo-devo, Pattern formation, Wing epithelium, Wnt signaling, Frizzled receptors, Morphogens, Planar cell polarity, Decoy receptor

[1]Department of Biological Sciences, The George Washington University, Washington, DC 20052, USA. [2]Smithsonian Tropical Research Institute, Gamboa 0843-03092, Panama. [3]Department of Biology, University of Puerto Rico at Río Piedras, San Juan 00931, Puerto Rico. [4]Department of Zoology, University of Cambridge, Cambridge CB2 3EJ, UK. [5]Epigenetics and Stem Cell Biology Laboratory, National Institute of Environmental Health Sciences, Durham, NC 27708, USA. [6]Department of Cell and Developmental Biology, UC San Diego, La Jolla, CA, USA. [7]Division of Evolutionary Biology, Ludwig Maximilian University, Munich 80539, Germany. [8]Molecular Sciences and Research Center, University of Puerto Rico, San Juan 00931, Puerto Rico. [9]Dipartimento di Scienze Chimiche della Vita e della Sostenibilità Ambientale, Università di Parma, Parma 43121, Italy.
*These authors contributed equally to this work

‡Author for correspondence (arnaud@gwu.edu)

J.J.H., 0000-0002-9459-9776; L.S.L., 0000-0003-0981-7984; A.M.-V., 0000-0001-9644-2871; T.S.R.-M., 0009-0004-6311-4600; L.L., 0000-0002-2597-7550; C.R.D., 0000-0002-1841-950X; N.L., 0009-0002-1697-3723; O.B.W.H.C., 0000-0003-4893-5211; J.A.A., 0009-0003-5313-7334; M.R., 0000-0001-9992-3355; R.P., 0000-0002-7986-9993; W.O.M., 0000-0003-2805-2745; M.W.P., 0000-0002-5977-8031; A.M., 0000-0002-5980-2249

Handling Editor: Cassandra Extavour
Received 12 April 2023; Accepted 4 August 2023

INTRODUCTION

The Wnt-family ligand WntA instructs color pattern formation during butterfly wing development and establishes the position and limits of color fields across Nymphalidae (Martin and Reed, 2014; Mazo-Vargas et al., 2017). Several lines of evidence pinpoint WntA signaling as a driver of color pattern evolution. First, regulatory shifts of *WntA* spatial expression have repeatedly driven adaptive variation, as evidenced by the identification to date of more than 20 *WntA* alleles associated with wing mimicry in variable species of the *Heliconius*, *Limenitis* and *Elymnias* butterfly radiations (Gallant et al., 2014; Martin et al., 2012; Morris et al., 2020; Ruttenberg et al., 2021; Van Belleghem et al., 2017), making *WntA* a favored genomic locus for wing pattern variation (Martin and Courtier-Orgogozo, 2017; Van Belleghem et al., 2021). In these systems, *WntA* alleles explain pattern differences between populations and morphs of the same species. Additionally, mapping, expression and loss-of-function experiments show that *WntA* repeatedly shaped the spectacular ressemblance of *Heliconius* co-mimics that converged onto identical patterns, in spite of historical drift in their patterning systems (Concha et al., 2019; Van Belleghem et al., 2020). Although *WntA* regulation and function appear largely conserved across butterflies that follow a bauplan-like organization of wing patterns known as the Nymphalid Ground Plan (NGP), it has also evolved atypical modes of expression associated with novel pattern elements, such as in the control of white-orange intravenous markings in the monarch butterfly (Mazo-Vargas et al., 2017, 2022). A high density of open-chromatin elements at this locus, each involved in the regulatory control of pattern phenotypes, may underlie the apparent evolvability of *WntA* expression in nymphalids (Mazo-Vargas et al., 2022).

In addition to the insights it provides on genetic evolution, *WntA* wing patterning also brings the opportunity to study morphogenetic signaling in a simplified, two-dimensional developmental system, where color states provide a direct phenotypic readout of positional information during development. Although *WntA* evolved at the base of Metazoa (Darras et al., 2018; Kraus et al., 2016; Somorjai et al., 2018), it was lost in vertebrates as well as in Cyclorrhapha, a fly lineage that includes *Drosophila* (Hanly et al., 2021), making it a particularly understudied Wnt ligand. CRISPR mosaic knock-outs of *Wntless* (*Wls*) and *porcupine* (*por*) phenocopy *WntA* knockouts, which implies that WntA is a secreted lipid-modified ligand that is processed via the classical Wnt secretory pathway (Hanly et al., 2021). In addition to its role in Wnt maturation and secretion, the fatty acid thumb added by Por-dependent acylation is essential for steric binding of Wnt ligands into the cysteine rich domains (CRD) of receptors of the Frizzled family (Alvarez-Rodrigo et al., 2023; Hoppler and Moon, 2014; Nile and Hannoush, 2019; Povelones and

Development (2023) 150, dev201868. doi:10.1242/dev.201868

Nusse, 2005). Studies of Wingless (Wg/Wnt1) in *Drosophila* development have shown that Frizzled1 and Frizzled2 (Fz1, Fz2) mediate short-range Wnt reception with different efficiencies, and that they are transcriptionally repressed by Wg signaling (Bhanot et al., 1999; Chen and Struhl, 1999; Moline et al., 2000). In the *Drosophila* wing disc, Fz1 is the sole Frizzled receptor necessary for the Wnt-independent Fz/planar cell polarity (Fz/PCP) pathway (Ewen-Campen et al., 2020); Fz2 maintains long-range activation of the Wnt pathway in cells that are beyond the reach of extracellular Wg (Chaudhary et al., 2019); Fz3 is a decoy receptor of Wg that attenuates signaling (Sato et al., 1999; Schilling et al., 2014); and Fz4 has no known function in wings (Ewen-Campen et al., 2020). In butterflies, a RNAseq study showed that the butterfly homolog of *frizzled2* (*fz2*) is differentially expressed across color regions during early pupal wing development (Hanly et al., 2019), and *in situ* hybridizations of the four frizzled gene homologs showed overlap with the expression of Wnt ligand genes (Banerjee et al., 2023).

To further shed light on the mechanisms of *WntA* reception, we have investigated functions of the Frizzled family seven-transmembrane domain receptors during butterfly wing development. Using CRISPR-mediated mutagenesis across several butterfly species of the Nymphalidae family, we show that *fz2* is the only Frizzled-family receptor required for the formation of WntA-dependent patterns. In contrast, *frizzled1* mosaic knockouts indicate it mediates a conserved Fz-PCP pathway involved in scale orientation. Finally, we show that loss of function of *frizzled3* (*fz3*) and *frizzled4* (*fz4*) play negative roles on WntA-independent Wnt signaling during wing development.

RESULTS

Nymphalid butterfly genomes encode four Frizzled receptors

Frizzled receptors are seven-transmembrane-domain proteins belonging to the G protein-coupled receptor family. Most non-vertebrate genomes encode four Frizzled orthology groups that originated before the Bilateria/Cnidaria split, including the four receptors annotated in *Drosophila* (Janssen et al., 2015; Schenkelaars et al., 2015). We recovered orthologues of these four genes in nymphalid butterfly genomes, hereafter numbered by orthology groups and abbreviated *fz1*, *fz2*, *fz3* and *fz4* (Fig. S1A, Table S6). Both *fz1* and *fz2* have a conserved KTxxxW motif (Fig. S1B), required for the recruitment of Dishevelled (Dsh), which relays two pathways in *Drosophila*: Fz1/2-dependent canonical Wnt signaling and Fz1/PCP signaling (Ewen-Campen et al., 2020; Gao and Chen, 2010; Mieszczanek et al., 2022; Tauriello et al., 2012). In addition, the KTxxxW is invariable between Fz2 orthologues between *Drosophila* and Lepidoptera, showing a conserved KTLESW peptidic chain with a predicted glutamyl-endopeptidase site, necessary for the Frizzled nuclear import (FNI) pathway in *Drosophila* (Mathew et al., 2005; Restrepo et al., 2022). In contrast, Fz4 lost its KTxxxW domain in both Lepidoptera and Diptera, and Fz3 shows a derived Thr>Ser substitution in position 2 of unknown functional relevance. Overall, amino acid sequences from the cytoplasmic domains suggest that nymphalid Frizzled receptors may function similarly to the dipteran model *Drosophila*, with Fz1/2 signaling via Dishevelled recruitment, Fz2 potentially subject to the FNI Wnt pathway and Fz3/4 playing alternate roles. *In situ* hybridization of the four fz orthologues of *V. cardui* show these four genes are expressed in wing imaginal disks from fifth instar larvae, but without an apparent association with color patterns, unlike *WntA* at this stage (Fig. S1C-G). These data suggest functional divergence in the use of Frizzled receptors in butterfly wing development.

Fz2 is required for WntA patterning across nymphalid butterflies

A previous RNAseq analysis in *Heliconius* pupal wings suggested spatial complementarity of *fz2* expression levels with *WntA* (Hanly et al., 2019). We thus sought to test the function of *fz2*, and used CRISPR somatic mutagenesis to generate mosaic knockouts (mKOs) of *fz2* in six species previously targeted for *WntA* mutagenesis (Concha et al., 2019; Mazo-Vargas et al., 2017, 2022).

In all instances, *fz2* mKOs phenocopied the effects of *WntA* loss of function, with the removal or shifts of specific patterns on all four wing surfaces. Specifically, the phenotypes observed in *V. cardui* and *J. coenia* show (1) complete loss of the central symmetry system (CSS) – a conserved pattern element that expresses *WntA* (Martin and Reed, 2014; Mazo-Vargas et al., 2017); (2) shifts in peripheral patterns; and (3) specific reductions or loss of other WntA-expressing patterns, such as the *V. cardui* forewing eyespots and the *J. coenia* Basalis orange-black pattern (Fig. 1A,C). In *A. incarnata*, *fz2* crispants reproduce all losses of silver spots known to express *WntA* in fifth instar wing disks, as well as an expansion of silver domains in the anterior hindwing, a phenomenon also observed in *WntA* mKOs (Martin and Reed, 2014; Mazo-Vargas et al., 2017). We knocked out *fz2* in a pair of *Heliconius* butterfly co-mimics that convergently evolved a red forewing band. The *fz2* mKOs recapitulated the species-specific effects of *WntA* removal (Concha et al., 2019; McMillan et al., 2020): a subtle proximal extension of the red band revealing a cryptic yellow dot in *Heliconius melpomene rosina*, versus an extensive proximal extension in *Heliconius erato demophoon*. Additionally, we repeated *WntA* mKOs in the monarch butterfly *Danaus plexippus* (Fig. S2), confirming that *WntA* evolved a role in antagonizing the formation of white patterns that outline black vein markings (Mazo-Vargas et al., 2017). Loss of function of *fz2* reproduced these effects, with white patterns expanding in these fields.

As observed in *WntA* mKOs, *fz2* mKOs generated by injection of a Cas9/sgRNA duplex in syncytial embryos resulted in healthy adult G_0 butterflies without detectable deleterious impacts on wing development (Figs S3-S6, Table S1). In particular, we did not observe the high rates of missing wings observed with *por* and *wls* mKOs (Hanly et al., 2021). This suggests that *fz2* alone is dispensable for mediating Wnt functions that are essential for normal wing growth, which parallels perturbation assays in *Tribolium* embryos and *Drosophila* wings, where *fz2* loss-of-function effects are phenotypically silent due to functional redundancy with *fz1* (Beermann et al., 2011; Ewen-Campen et al., 2020). However, *fz2* crispants showed highly efficient and penetrant wing color pattern phenotypes in all tested species (Fig. 1).

A closer look at *WntA* and *fz2* crispants reveals interesting differences in the shape and aspect of mosaic clones (Fig. 1G-J). *WntA* clones always appear rounded: this is consistent with the expected non-cell-autonomous effects of a paracrine signaling ligand. In contrast, *fz2* clones show elongated jagged shapes in the proximo-distal direction, consistent with expectations for cell-autonomous effects, and reminiscent of the shape of butterfly wing clones obtained with mKOs of selector transcription factors and pigment pathway genes (Livraghi et al., 2018; Tunström et al., 2023; Westerman et al., 2018; Zhang et al., 2017a,b), which we would also expect to be cell-autonomous. Taken together, these data show that Fz2 reception is necessary for mediating WntA patterning, and that WntA signals reach several cell diameters away from their source.

WntA signaling represses *fz2* expression in pupae

Together, the WntA ligand and Fz2 receptor form a paracrine signaling axis required for the induction of CSS patterns, as well as

Development (2023) 150, dev201868. doi:10.1242/dev.201868

Fig. 1. CRISPR-induced *fz2* mKOs phenocopy *WntA* mKOs in six nymphalid species, but in a cell-autonomous rather than non-cell-autonomous fashion. (A-F) Ventral views comparing the effects of *WntA* and *fz2* mKOs in individuals with extensive phenotypes, i.e. with no or little mosaicism, except in monarchs, where no fully penetrant *fz2* phenotype was obtained (F, right panel). *WntA* crispants shown in B-D were generated in previously published studies (Concha et al., 2019; Mazo-Vargas et al., 2017). (G-J) Magnified views of mutant clones in individuals with high mosaicism, contrasting the non cell-autonomy of *WntA* mKOs (rounded boundaries) with the cell-autonomy for *fz2* (jagged boundaries with conservation of pattern layers). (G,H) Ventral forewings with magnified views of the M_3-Cu_2 region in *A. incarnata* (G) and Cu_2-Cu_1 in *D. plexippus* (H). (I,J) Ventral hindwings with magnified views of the M_3-Cu_2 region in *A. incarnata* (I) and Cu_2-Cu_1 in *D. plexippus* (J). Scale bars: 1 mm.

for the proper positioning of pattern elements close to the wing margin, such as the distal Parafocal elements (dPf), Marginal Band System (MBS) and the WntA-dependent forewing Border Ocelli (fBOc) in *V. cardui* (Fig. 2A, Figs S7 and S8A-C). *In situ* hybridization in a number of species had previously shown that *WntA* expression already prefigures pattern elements in late larval wings (Jiggins et al., 2017; Martin and Reed, 2014; Mazo-Vargas et al., 2017). However, current evidence suggests that extracellular WntA signaling mostly occurs in pupal rather than in larval wings. Indeed, injections of heparin, an extracellular Wnt interactor that results in Wnt-dependent pattern expansions (Martin and Reed, 2014; Mazo-Vargas et al., 2017; Sourakov, 2018; Sourakov and Shirai, 2020), are effective in the first 15% of pupal development – typically within 24 h after pupa formation (APF) at optimal rearing temperatures. Furthermore, scale organ precursor cell differentiation occurs around 13-15% (Dinwiddie et al., 2014), and the competency of tissue grafts to induce ectopic patterns (Nijhout, 1991) or developmental studies of eyespot formation (Brunetti et al., 2001; Monteiro, 2015), all imply the existence of paracrine signals active during early pupal development. We thus hypothesized that extracellular WntA signaling function actually occurs after the onset of metamorphosis.

We examined *WntA* and *fz2* mRNA expression in early pupal wings in order to gain further insights into WntA/Fz2 patterning (Fig. 2, Fig. S8). Consistent with an instructive role for pattern induction in pupal wings, *WntA* expression precisely prefigured the

Development (2023) 150, dev201868. doi:10.1242/dev.201868

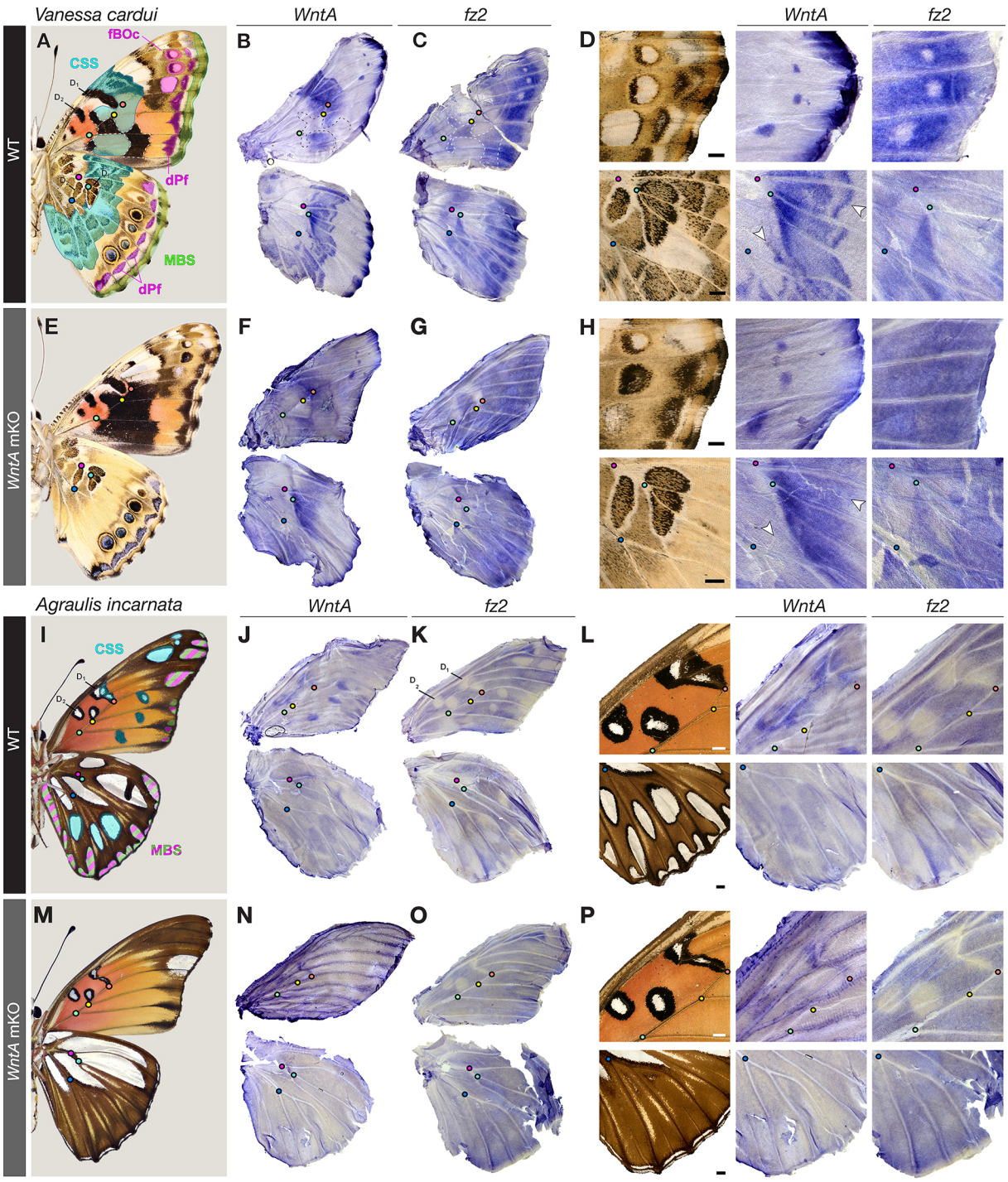

Fig. 2. Expression of *WntA* and *fz2* in pupal wings is under the control of positive and negative feedback. (A) Ventral *V. cardui* annotated with its main pattern homologies from the nymphalid groundplan (NGP): D_1 and D_2, Discalis elements; CSS, Central Symmetry System (cyan); MBS, Marginal Band System (green). The Border Ocelli Symmetry System (BoSS, magenta) consists of the following: fBOc, forewing Border Ocelli; dPf, distal Parafocal elements. Colored dots mark vein intersection landmarks (magenta and turquoise, R veins; red, crossvein-M_3; yellow, M_3-Cu_1; green and blue, Cu_1-Cu_2). (B-D) *In situ* hybridization for *WntA* and *fz2* mRNA in wild-type *V. cardui* wings, and magnified views in the anterior tip of the forewing (top) and medial hindwing (bottom). (E-H) Equivalent experiments to those in A-D following *WntA* knockout. Arrowheads point at pattern elements that are disrupted in the mKO condition compared with WT (D,H). (I) Derivation of the NGP in ventral *A. incarnata*. The CSS is dislocated and marginal patterns may include partial homology with dPf elements (green and magenta). (J-L) *In situ* hybridization for *WntA* and *fz2* mRNA in wild-type *A. incarnata* wings with magnified views of the anterior tip of the medial forewing (top) and hindwing (bottom). (M-P) Expression assays (similar to J-L) after *WntA* knockout. Comparisons of *WntA* versus *fz2* in *V. cardui* (B-D,F-H) are shown in contralateral tissues from the same individual. Scale bars: 1 mm.

position and shape of WntA-dependent pattern elements, including delineations of the adult patterns and graded expression levels that prefigure their textural details in a more highly correlated way than in larvae, in all species examined. (e.g. Fig. 2D, Fig. S8F). On the other hand, *fz2* is generally expressed in an anti-correlated pattern with *WntA*. In *A. incarnata*, as in *V. cardui*, we found

Development (2023) 150, dev201868. doi:10.1242/dev.201868

complementary expression of *fz2* and *WntA* in pupal stages in wild-type wings (Fig. 2F-K). In summary, *fz2* showed complementary expression to *WntA,* with low staining in *WntA*-positive regions across all the wild-type tissues we assayed. This is indicative of WntA-dependent repression of *fz2* expression in the nymphalids, a phenomenon observed with Wg and *fz2* in larval *D. melanogaster* wing discs (Cadigan et al., 1998; Zhang and Carthew, 1998).

In order to test whether WntA represses expression of *fz2*, we performed *fz2* mRNA *in situ* hybridization in *WntA* G_0 mosaic knockouts of *V. cardui* and *A. incarnata.* In both species, patterns of *fz2* expression were markedly affected by *WntA* KO, and all WntA-expressing patterns lost the local repression of *fz2* (Fig. 2E-H, Fig. S8H,I,L,M). The local repression of *fz2* requires a functional WntA. Thus, although Fz2 is a positive regulator of WntA signaling, *fz2* expression is also repressed by WntA, and this mechanism is likely to enforce a transcriptional negative-feedback loop on this pathway.

Fz2 mediates the patterning functions of other Wnts

The mRNA signal for *fz2* remained low in D_1 and D_2 Discalis patterns in the WntA-deficient wings of the two species we assayed (Fig. 2H,P), implying that a WntA-independent signal repressed *fz2* in these patterns. In parallel, a closer examination of these phenotypes reveal that *fz2* KOs consistently induced black pattern expansions in *V. cardui* forewing D_1 and D_2 (Fig. S9A). This effect is not detected in *WntA* KOs, implying that Fz2 receives additional patterning signals from other ligands in this part of the wing. In the *V. cardui* forewing, this may include Wg, as D_1 and D_2 express both *wg* and *WntA* (Fig. S9A-G). We infer that Fz2 mediates the patterning functions of Wg or another Wnt, and may be under additional negative transcriptional feedback from this input, similar to WntA in other color patterns, or to the Wg/Fz2 pair in *Drosophila* (Cadigan et al., 1998; Chaudhary et al., 2019; Schilling et al., 2014). On the other hand, in the two nymphalids *A. incarnata* and *J. coenia* (Figs S9H,I and S10), *wg*-positive patterns (Martin and Reed, 2010, 2014), such as the D_2 element, are unaffected by the *fz2* KO, suggesting that if Fz2 is necessary for Wg color patterning, it must be redundant with another receptor in some contexts or species.

WntA signaling feedback refines *WntA* expression

In addition to the transcriptional negative feedback on *fz2*, our data also suggest that *WntA* expression is under the control of positive feedback. This effect is most visible in the CSS patterns of *V. cardui*, where the spatial complexity of *WntA* pupal expression disappears when WntA signaling is removed. For example, *WntA* expression in wild-type hindwings prefigures textural details of the CSS, with sharp outer boundaries, and a complex composition of undulating patterns in between (Fig. 2D, bottom row). These features of *WntA* expression are lost upon *WntA* KO (Fig. 2H, bottom row), meaning that a positive feedback of WntA signaling likely refines the sharply delineated and undulatory aspect of the ventral hindwing CSS in *V. cardui*. Similarly, in the wild-type posterior forewing, *WntA* is expressed in wide blocks that mark the presumptive orange patterns (Fig. S8G). In WntA-deficient pupal forewings, i.e. in the absence of a WntA positive-feedback loop, *WntA* expression is depleted from the inside of these patterns but remains high in two continuous lateral lines (arrowheads in Fig. S8G).

Elsewhere, *WntA in situ* hybridization shows reduced staining following *WntA* mKO in *V. cardui* and *A. incarnata* marginal patterns, as well as in the *A. incarnata* CSS (Fig. 2, Fig. S8), indicating the existence of feedback mechanisms. As an exception, *WntA* expression in the *V. cardui* forewing eyespots appears unchanged upon mKO and may be largely WntA independent (Fig. 2D,H, upper rows). In summary, the shifts in *WntA* expression observed in loss-of-function crispants indicate that positive feedback is necessary for the elaboration of CSS features in *V. cardui* wings. The importance of this feedback may vary across regions and species.

WntA/Fz2 signaling provides proximodistal positioning to peripheral patterns

The patterns closest to the wing margin consist of stripe patterns that form the MBS as well as the dPf, a pattern often taking the shape of individuated arcs or chevrons between each wing vein compartment (Nijhout, 2017; Otaki, 2012; Taira et al., 2015). *WntA* is strongly expressed at the vein tips of *V. cardui* pupal hindwings (Fig. 3A). Transcripts of *fz2* are repressed across a larger domain across the periphery, suggesting local repression by negative feedback from marginal signals (Fig. 3B). *WntA* mKOs leave border ocelli (eyespots) and MBS patterns unaffected in this system (Hanly et al., 2021; Mazo-Vargas et al., 2017), but result in a visible shift and reversal of the dPf blue chevron shapes (Fig. 3C,D). These phenotypes are reproduced in *fz2* crispant butterflies, with dPf elements showing distalization and thickening (Fig. 3E). Unlike *WntA*-dependent continuous clonal effects of dPf elements, clonal mosaics of *fz2* KO result in apparent cell-autonomous gains of blue scales (Fig. 3D′,E′). Similar effects are visible in monarchs (Fig. 1H), where *WntA* and *fz2* are required for establishing the black contours of marginal white spots. Together, these expression and loss-of-function data suggest that *WntA* diffuses away from the vein tips and requires *fz2* for proper positioning and shaping of the dPf elements.

Inverted expression and patterning activity of WntA and Fz2 signaling across the M_2 vein in *A. incarnata*

The wing patterns of *A. incarnata* present an interesting conundrum on the ventral hindwing. As described above, WntA and Fz2 are both necessary for the induction of most CSS and peripheral silver patterns (Fig. 3F-J′). However, knockouts of both genes result in an expansion and gain of silver spots (Fig. 1E) – for example, the large silver element situated in the anterior compartment (anterior to the M_2 vein) is normally split into two disjunct silver spots (dotted lines in Fig. 3M), whereas these spots fuse and extend basally in *WntA* and *fz2* KOs. Similarly, the M_1-M_2 region (above the green line in Fig. 3M) normally lacks silver elements, but shows an ectopic silver pattern in these crispants. Why are there two opposed effects of WntA on silver spots? Surprisingly, we found that *WntA* expression is absent from the anterior silver spots, and is instead expressed in their brown contouring regions in pupal wings (Fig. 3K-N). WntA signaling is notably active in the domain that splits the M_1-M_2 region into two spots, as observed by strong *WntA* and low *fz2* mRNA patterns, and decreased signaling results in silver spot extensions. In other words, although WntA/Fz2 generally activates silver and black outlines in *A. incarnata* ventral surfaces, it can also locally shift to a complementary expression mode that induces the brown contours of similar patterns instead. These data establish WntA/Fz2 signaling as a versatile developmental tool for setting boundaries in a context-dependent fashion, with the capacity to induce elements that are variably perceived as ‘pattern’ or ‘background’ (Nijhout and Wray, 1988).

Development (2023) 150, dev201868. doi:10.1242/dev.201868

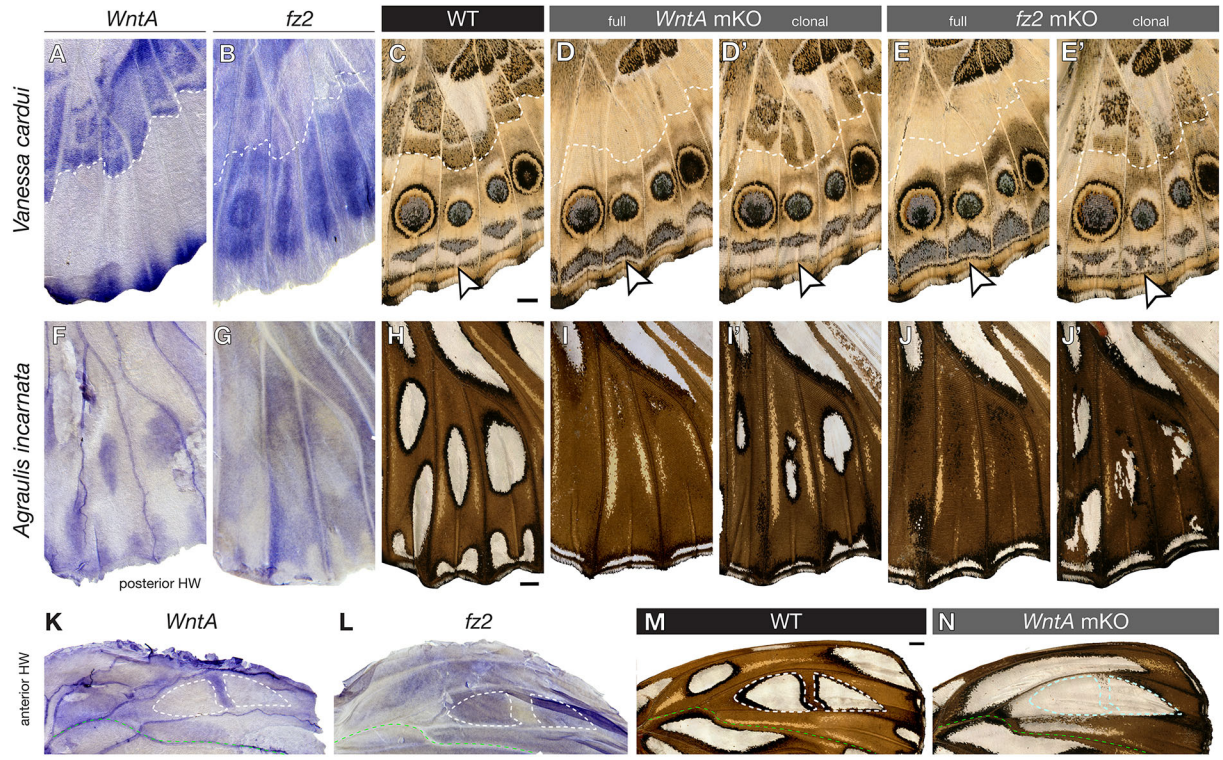

Fig. 3. WntA/Fz2 signaling in the formation of ventral hindwing patterns. (A,B) In *V. cardui* pupal wing mRNA staining, *fz2* is repressed in regions of high WntA signaling away from the wing margin (bottom). (C-D′) *WntA* mKOs show a distal shift of the blue dPf chevrons towards the submarginal band pattern (arrowheads). Wings with high mosaicism in the CSS (above the dotted line) show undulating chevrons in the dPf (D′). (E,E′) *fz2* mKOs phenocopy the distalization of dPf elements (arrowheads) seen in *WntA* mKOs. The irregularity of mosaic clones suggests cell-autonomy (E′). (F,G) WntA-Fz2 signaling is active in presumptive CSS and marginal silver patterns of the posterior hindwing in *A. incarnata*. (K-N) Reversed deployment of WntA signaling around anterior silver spots in *A. incarnata* hindwings, explaining the expansion of silver spots (white dashed outlines) in *WntA* KOs (N) that are anterior to the M_2 vein (green dashed line). Scale bars: 1 mm.

Fz1 loss of function results in planar cell polarity-like effects

Next, we assayed the other three Frizzled receptors for effects on development and wing patterning. First we generated *fz1* mKO across a large sample of *J. coenia* embryos (n=5273), varying injection time and CRISPR duplex concentration, and testing two different sgRNA targets. We did not observe pattern effects in these butterflies, but instead, crispants showed disorganized arrays of scales that were most conspicuous on the wings and antennae (Fig. 4A-C′, Fig. S11). These effects are clonal (i.e. with visible boundaries between mutant and wild-type scale fields), and reminiscent of *Drosophila* PCP phenotypes (Adler, 2012; Lawrence and Casal, 2018): similarly to wing hairs in PCP mutant flies, *fz1*-deficient butterfly scales are globally misoriented, forming streaks of scales that deviate from the normal proximal-to-distal orientation. Mutant scales also showed upright positions relative to the wing plane, indicative of a loss of the asymmetry normally observed in the scale protrusion axis during early pupal development (Dinwiddie et al., 2014). Mosaic knockouts of *fz1* in *V. cardui* did not generate color pattern or scale defects among emerged adult butterflies (Table S1). However, in contrast to *J. coenia*, some pupae from this experiment showed wing growth defects and failed to form a cuticular seal with the abdomen, resulting in pupal death or failure of imago emergence due to desiccation (Fig. S12). Additionally, in the *J. coenia* crispants that showed PCP phenotypes on one side only (Fig. S13), mutant forewings were shorter and rounder than their wild-type counterparts (Wilcoxon signed rank test, P<0.05). This suggests that although *fz1* deficiencies can also affect wing growth in *J. coenia*, pupal viability is less sensitive to perturbation in this species than in *V. cardui*.

To further verify its link to scale polarity, we used siRNA electroporation to generate knockdowns of *fz1* at the pupal stage (Fujiwara and Nishikawa, 2016; VanKuren et al., 2023), thus bypassing the wing growth phase from larval stages. Electroporated siRNA knockdowns consistently recapitulated PCP phenotypes in *J. coenia* and *A. incarnata* (Fig. 4C,G-J). In each butterfly, these effects were specific to the electroporated surface, and were not observed in sham-treated controls targeting a GFP sequence (Fig. S14). In *J. coenia*, we also reproduced hindwing-to-forewing pattern homeoses by knocking down the *Ultrabithorax* Hox gene (Tendolkar et al., 2021), as well as by local removal of the CSS using *fz2* knockdowns (Fig. S15). These two positive controls both reproduced expected effects and show that the PCP-like effect is not induced as an artifact of electroporation. Thus, the combination of CRISPR KOs and siRNA knockdowns indicate the conservation of a Fz1-PCP pathway required for the proper orientation of epithelial features, similar to *Drosophila* (Ewen-Campen et al., 2020; Joyce et al., 2020).

Fz3 and Fz4 are inhibitors of vein formation

Next, we found that mosaic knockouts of both *fz3* and *fz4* in *V. cardui*, *J. coenia* and *A. incarnata* generated similar effects on vein and color patterning (Fig. 5A-C, Figs S16-S20). Most notably, disruption of *fz3* and *fz4* results in ectopic veins across all wing surfaces, sometimes forming complete veins and sometimes forming short spurs or loops (Fig. 5D), showing that these two

Development (2023) 150, dev201868. doi:10.1242/dev.201868

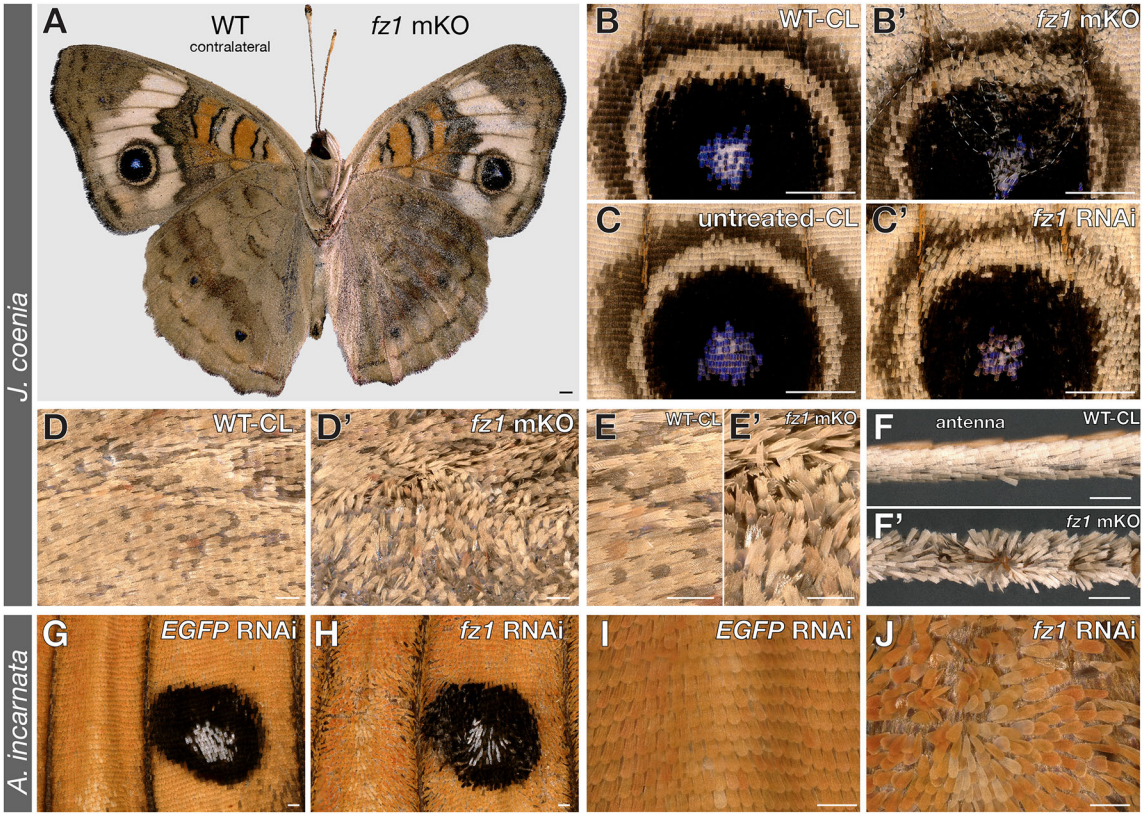

Fig. 4. PCP-like scale orientation defects in *fz1* mKO and RNAi knockdowns. (A) *J. coenia fz1* crispant with mutant phenotypes limited to a single side (A, right; magnified in B,D,E), and a contralateral wild-type (WT-CL) side (A, left; magnified in B′,D′,E′,F′). (B,B′) PCP-like clones in the Cu_1 eyespot from *fz1* mKO clones. (C,C′) Mild PCP-like phenotypes observed in electroporated RNAi experiments targeting *fz1*. (D-E′) Magnified view of an anterior forewing region comparing *fz1* mKO with WT-CL scales. WT-CL images were horizontally flipped to match the crispant wing direction. (F,F′) Scale orientation defects on antennae, as seen here in the asymmetric *fz1* crispant (A). (G-J) Strong PCP-like phenotypes observed after *fz1* siRNA electroporation in *A. incarnata* (n=8), compared with sham controls targeting an EGFP sequence (n=2). The Cu_1-M_3 ventral forewing CSS silver spot is shown in G,H. Limb orientations: B-C′ and G-J, distal at the bottom; D-F′, distal on the right. Scale bars: 1 mm in A-C′; 200 µm in D-J.

genes have non-redundant roles in the repression of vein formation. As the lacunae, which prefigure the veins, form during larval wing development, this vein inhibition function is likely to occur before metamorphosis (Banerjee and Monteiro, 2020; Nijhout, 1991; Reed and Gilbert, 2004; Reed et al., 2007). Consistent with this idea, *fz3* and *fz4* are expressed in the intervein regions of *V. cardui* larval wing discs (Fig. S1). In places where a supernumerary vein interacted with the eyespot field in *V. cardui* and *J. coenia*, we observed alterations to the shape and size of eyespots, including the formation of additional eyespot foci (Fig. 5E, Figs S16-S19). Veins act as important signaling centers and domain boundaries (Connahs et al., 2019; Nijhout, 2017), and ectopic foci may thus be a secondary consequence of ectopic veins, rather than a direct interaction between Fz3 and/or Fz4 and eyespot-inducing morphogens. Likewise, disruptions of CSS elements were accompanied by ectopic venation (i.e. Fig. 5A″), suggesting a collateral effect of venation on field boundary conditions rather than on the WntA morphogen itself.

Differential roles of Fz3 and Fz4 in color patterning and wing margin specification

We further examined possible color patterning functions of *fz3* and *fz4*, with their confounding effects on venation in mind. In *J. coenia* and *A. incarnata*, Discalis elements are bicolor symmetric systems and express Wnt ligand genes such as *wg* (Figs S4I and S5B), *Wnt6* and *Wnt10* (Martin and Reed, 2014), and *WntA*, although the last only contributes to the patterning of *A. incarnata* D_1 (Mazo-Vargas et al., 2017). Both *fz3* and *fz4* showed expansions of Discalis elements (Fig. 5F-G). These effects of *fz3* perturbation are again likely to derive from ectopic venation, as they are accompanied by visible epithelial thickening in these regions or as they formed close to other veins that may have formed spurs. Interestingly, *fz4* mKOs had distinct effects that suggest a direct modulation of pattern-inducing morphogenetic signals, rather than a collateral effect of ectopic venation. In *fz4* crispants, D_1 and D_2 had expanded inner and outer elements on the ventral side, whereas on the dorsal side, only the outer black element was expanded (Fig. 5F,G). Unlike *fz3* phenotypes, these expansions appear broader and always include a graded, fuzzy effect at their borders, suggesting a possible non-cell-autonomous effect on extracellular signaling.

Observation of the wing peripheral regions of *J. coenia* and *V. cardui* provide further insights (Fig. 6), as they juxtapose a sequence of multicolor patterns (dPf and MBS) with possible contributions of WntA and Wg, Wnt6 or Wnt10 (Martin and Reed, 2014; Mazo-Vargas et al., 2017). Perturbation of *fz4* yields specific effects on MBS patterning, seen as a loss of the sub-marginal band in *J. coenia* and an MBS distal shift or reduction in *V. cardui,* as well as a distalization of eyespots observed in *V. cardui* only (Fig. 6A,B,D,E,G,H). In contrast, the color pattern arrangements of *fz3* crispants are similar to wild type in complexity (i.e. similar sequences and sizes of color layers), but instead show distortions

Development (2023) 150, dev201868. doi:10.1242/dev.201868

Fig. 5. Effects of *fz3* and *fz4* mKOs on wing venation and color pattern formation. (A-C″) Dorsal (left) and ventral (right) views of representative mosaic crispants for *fz3* and *fz4* in three species. Arrowheads indicate color pattern defects explained by ectopic venation; double-headed arrows indicate non-cell-autonomous color pattern defects observed without (A″,B″) or in conjunction with (C″) ectopic venation. (D) Both *fz3* and *fz4* mKOs induce ectopic veins (arrowheads), shown here in descaled *V. cardui* forewings. (E) Split eyespots observed in *fz3*/*fz4* crispants result from ectopic venation. Dashed lines indicate wing veins. (F,G) Ventral and dorsal Discalis pattern aberrations in *J. coenia* and *A. incarnata*. *fz3* crispants show irregular Discalis patterns with sharp boundaries, seemingly associated with ectopic venation (arrowheads). *fz4* mKO results in expansions of Discalis patterns with unsharp boundaries (double-headed arrows), suggesting non-cell-autonomous effects on extracellular morphogens, and ectopic patterns associated with ectopic venation (arrowheads). Arrowheads in D-G indicate ectopic veins. Scale bars: 2 mm.

that indicate two kinds of tissue distortions: ectopic venation and ectopic wing margins. These secondary wing margins are visible as distal outgrowths that feature the sequence of scale types normally found at the primary margin, including linear streaks of elongated margin scales (Fig. 6C,F,I). Together with the strong expression of *fz3* in the peripheral tissue of larval wing disks (Fig. S1F), these results suggest that *fz3* is necessary for proper margin specification.

Development (2023) 150, dev201868. doi:10.1242/dev.201868

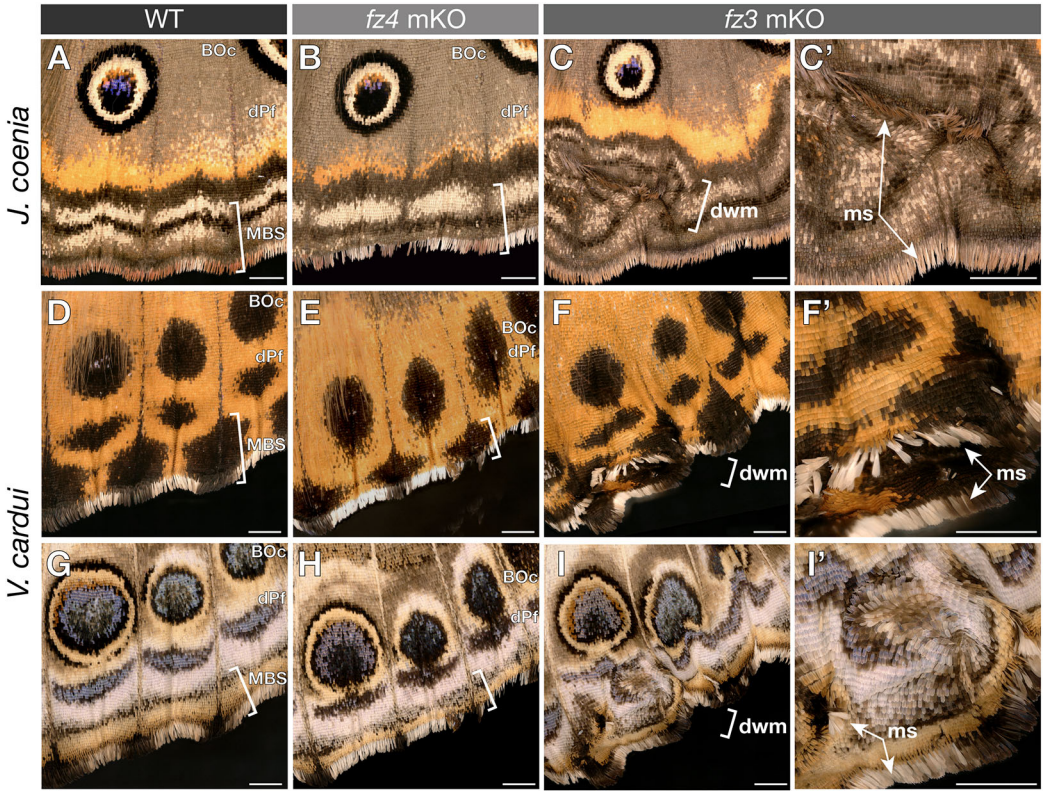

Fig. 6. Peripheral effects of *fz4* and *fz3* mKOs on color patterns and the wing margin. (A-C′) Dorsal views of *J. coenia* crispants, with reduced MBS patterns in *fz4* mKOs and localized distortions of the wing margin in *fz3* mKOs. In *fz3* mKOs, margin scales (ms, arrows) and concentric layering of color patterns and scale types around them indicate the presence of duplicated wing margins (dwm, magnified in C′,F′,I′), in addition to ectopic veinous tissue. (D-I′) The same observations in the dorsal (D-F′) and ventral (G-I′) sides of *V. cardui*, with the added finding that eyespots (Border Ocelli, BOc) are distally shifted and collapsing with the distal Parafocal (dPf) chevron elements in *fz4* crispants of this species. Scale bars: 1 mm.

DISCUSSION

The WntA-Fz2 signaling axis instructs wing pattern formation

Here, we showed that Fz2 is the sole Frizzled-family member necessary for WntA reception in butterflies. Importantly, both *WntA* and *fz2* knockouts result in viable embryos, larvae and adults, without deleterious effects on survival or morphology, in spite of complex expression patterns (Hanly et al., 2021; Janssen et al., 2015). These results are in agreement with loss-of-function experiments in *Tribolium*, where knockdowns of *WntA* and *fz2* alone have no effect on embryogenesis (Beermann et al., 2011; Bolognesi et al., 2008), or in *Drosophila*, where null-homozygous *fz2* mutant adults are sterile but viable (Chen and Struhl, 1999; Cohen et al., 2002).

In addition, we gained insight on how *WntA*-dependent elements establish symmetric and complex arrays of color scales, such as the undulating brown patterns of the *V. cardui* CSS or the *A. incarnata* silver spots and their black contours (Figs 2,3). We propose that WntA acts as a morphogen, inducing scale cell differentiation in a graded and concentration-dependent manner. First, WntA acts as a paracrine factor, as indicated by the non-cell-autonomous nature of *WntA* crispant clones, with rounded boundaries that contrast with the expected cell-autonomous feature of receptor-deficient clones in all species (Figs 1G-J and 3). Second, mRNA staining intensities prefigure the differentiation of scales into multiple different types. For example, we see spatially intricate expression signals of *WntA* in the *V. cardui* hindwing ventral CSS, where wild-type patterns display symmetric arrangements of beige, black, white and brown scales that disappear in WntA KOs (Fig. 3C-E). In *A. incarnata* *WntA* KOs, the non-cell-autonomous clonal effects we observed, such as the contraction of black-contoured silver spots into black spots, indicate a lower signaling level (Fig. 1G,I). This contraction is not observed in the corresponding patterns carrying cell-autonomous *fz2* mKO clones, where dislocated patterns display both silver and black scales. These distinct phenotypes are consistent with receiving cells responding to specific thresholds in extracellular levels of WntA, or to duration of exposure, and rule out sequential induction models involving intermediate signals (Iwata and Otaki, 2019). Together, the ability of WntA to act at a distance and to cause differentiation into multiple concentration-dependent cell types indicate that it is a bona fide morphogen.

We also observed localized depletion of *fz2* expression in WntA-dependent patterns, and a reduction of this effect upon *WntA* KO, showing that WntA/Fz2 high-level signaling triggers a negative feedback on *fz2* mRNA expression. We found that *WntA* expression is under positive feedback, a phenomenon that may locally amplify signal and notably refine expression levels that prefigure color outputs in the *V. cardui* CSS (Fig. 2A-H). This pathway-intrinsic dual feedback mirrors aspects of Wg/Fz2 regulation in the *Drosophila* wing disk, and is generally thought to mediate precise and robust developmental signaling (Lander, 2007; Mehta et al., 2021; Sagner and Briscoe, 2017). These results lay out an exciting avenue of research for studying the formation of discrete responses for graded input in the butterfly wing, an epithelial tissue that effectively ‘displays’ differentiated cell states as scale colors.

Development (2023) 150, dev201868. doi:10.1242/dev.201868

Insights into Wnt pathway branching: a potential mechanism for wing modularity

In order to achieve the modular organization of pattern, butterfly wings are thought to deploy distinct cell signaling pathways and selector genes that control discrete sets of patterns in a region-specific manner (Martin and Reed, 2014; McKenna et al., 2020). As multiple Wnt ligand genes are expressed in butterfly wing transcriptomes (Fenner et al., 2020; Hanly et al., 2019), it is important to elucidate how many Wnt pathways are active in color patterning or, in other words, whether different branches of the Wnt transduction mechanisms can mediate separate cellular responses. Strikingly, *WntA* and *fz2* KOs remove the brown CSS in *J. coenia* but leave intact the overlapping, distinctively colored and *wg* positive D_1 and D_2 (Fig. S5) that are thought to be induced by Wg, Wnt6 and Wnt10 (Martin and Reed, 2014; Mazo-Vargas et al., 2017). This suggests that different Wnt signals diverge in their effects across the wings and induce distinct responses, with WntA most noticeably inducing the CSS and dPf, and Wg, Wnt6 and Wnt10 patterning D_1-D_2 and MBS elements. However, the distinctiveness of these elements would be difficult to explain if color-patterning Wnt pathways converge on the same transduction mechanism. This leads us to the working hypothesis that the WntA/Fz2 pathway is non-canonical, potentially separating its signal from canonical Wg activity in different sets of patterns. Non-canonical Fz2 pathway branches have been identified in *Drosophila* and will deserve further examination in butterflies to test this possibility, with candidate mechanisms including PTK7 family co-reception (Linnemannstöns et al., 2014; Peradziryi et al., 2011), ROR-family co-reception (Ripp et al., 2018; Shi et al., 2021), Fz2/Ca^{2+} signaling (Agrawal and Hasan, 2015) and the FNI pathway (Mathew et al., 2005; Restrepo et al., 2022).

Evolutionary conservation of the Wnt-independent Fz1-PCP pathway

Individual knockouts of Fz1 and Fz2 failed to disrupt Wg-positive patterns, suggesting that Fz1 and Fz2 act redundantly to mediate canonical Wg functions in butterflies, similarly to *Drosophila* and *Tribolium* (Beermann et al., 2011; Cadigan et al., 1998; Ewen-Campen et al., 2020). Nonetheless, *fz1* knockouts and knockdowns in several species showed that it is necessary for epithelial polarity, with phenotypes displaying disorganized scale arrays, akin to the wing trichome phenotypes characteristic of PCP in fruit flies (Adler, 2012). As in *Drosophila* (Ewen-Campen et al., 2020; Joyce et al., 2020), Fz1/PCP is independent of Wnt activity in butterflies, because knockouts of the Wnt secretion factors Wls and Por do not yield scale polarity defects (Hanly et al., 2021). These data validate previous inferences that this pathway is functionally conserved across Bilateria and Cnidaria (Momose et al., 2012; Yang and Mlodzik, 2015), and prompt further studies of Wnt-independent Fz1/PCP in a wider variety of arthropods and tissue types. Future investigations of butterfly wing PCP in particular could look at the effect of *fz1* mutation on scale and socket precursor orientation, cytoskeleton distribution, and asymmetry of the PCP marker Prickled during the first phases of pupal wing development (Adler, 2012; Day et al., 2019; Dinwiddie et al., 2014).

Fz3 and Fz4 are candidate Wnt pathway antagonists

The expression patterns of *fz3* and *fz4* in arthropod embryos are diverse, but imply ancestral roles in nervous system and appendage patterning (Janssen et al., 2015). In *Drosophila,* Fz3 acts as a decoy receptor, i.e. as a competitive-antagonist that attenuates Wnt signaling and contributes to establishing the Wg gradient in wing discs (Sato et al., 1999; Schilling et al., 2014). Of note, *fz3* is lost from the genomes of *Tribolium* beetles and *Parasteatoda* spiders (Janssen et al., 2015), and the developmental functions of Fz4 remain elusive in *Drosophila* and *Tribolium* (Beermann et al., 2011; Ewen-Campen et al., 2020).

Here, we show that both *fz3* and *fz4* play key roles in the formation of normal venation in the developing butterfly wings. Clonal knockouts had sporadic ectopic vein branching, implying that these genes are acting to repress vein development. No such role has been described in the literature for Fz3 or Fz4 in *D. melanogaster* wings (Ewen-Campen et al., 2020; López-Varea et al., 2021a). Despite this, activation of canonical Wnt signaling via misexpression of *wg* or of a constitutively active Arm induces ectopic veins in flies (Brennan et al., 1999; Lunde et al., 2003; Zeng et al., 2008), and knockdowns of the Wnt pathway genes *pegasus*, *Earthbound*, *pygopus* and *nemo* result in wing venation defects (López-Varea et al., 2021a,b), overall suggesting that the Wnt pathway is indeed a modulator of vein formation in flies.

Similarly, we found that *fz3* is strongly expressed in the wing periphery and that its loss-of-function results in ectopic wing margin duplications (Fig. 6). Lepidopteran wing disks develop with their dorsal and ventral epithelia in apposition, and form a wing margin that separates pre-apoptotic peripheral tissue from the wing epithelium (Macdonald et al., 2010; Nijhout, 1991). The Wnt ligand genes *wg*, *Wnt6* and *Wnt10*, as well as the transcription factor Cut, mark the peripheral tissue, analogous to the dorso-ventral (D-V) wing boundary characterized in flies (Gieseler et al., 2001; Macdonald et al., 2010; Swarup and Verheyen, 2012). Analogous to the role of canonical Wnt signaling in specifying the D-V boundary in flies (Buceta et al., 2007; Swarup and Verheyen, 2012), it is plausible that the *fz3*-deficient secondary margins we observed in butterflies result from a Wnt signaling gain of function.

Fz4 acts as a decoy Wnt receptor

A recent study suggested that butterfly Fz4 represses canonical Wnt signaling intracellularly in larval wings, and that it activates canonical Wnt signaling as well as Fz/PCP at pupal stages (Banerjee et al., 2023). Our data support the proposed Wnt antagonist role. However, we also found that Fz4 lost its KTxxxW domain in Diptera and Lepidoptera (Fig. S1), which makes it unlikely to recruit Dsh and thus to relay canonical Wnt and PCP signaling at later stages (Butler and Wallingford, 2017; Gao and Chen, 2010; Strutt et al., 2012). Instead, we propose that Fz4 acts as a decoy receptor that attenuates the amount of free Wnt ligands, by binding them without being structurally capable of transmitting a signal. In this model, Fz4 mKO leads to higher Wnt pathway activity and thus the induction of ectopic veins, and, in *Bicyclus*, of ectopic eyespots (Banerjee et al., 2023). A similar mechanism may explain the effects of *fz4* knockout on Discalis and MBS pattern elements. Specifically, the inner Discalis patterns (orange in *J. coenia*, silver in *A. incarnata*) expanded on ventral surfaces, while the outer black contours expanded in these same patterns on dorsal sides (Fig. 5F,G). In the peripheral patterns of both *V. cardui* and *J. coenia*, we observed a distal shift of eyespots accompanied by a simplification of the MBS patterns. Both Discalis and peripheral pattern aberrations from *fz4* crispants in three species showed rounded rather than jagged, irregular clones with sharp color breaks at boundaries (Figs 5F,G and 6). We interpret these effects as non-cell-autonomous, contrary to what would be expected from a classic receptor, but consistent with a Wnt decoy function occurring upstream of signal transduction, in the extracellular space. It is worth noting that *fz4* mKOs resemble the effect of extracellular

Development (2023) 150, dev201868. doi:10.1242/dev.201868

heparin injections in early pupae, a treatment that emulates Wnt gain of function, including Discalis element expansions, as well as MBS pattern fusion and expansions in *J. coenia, V. cardui* and *A. incarnata* (Martin and Reed, 2014; Serfas and Carroll, 2005; Sourakov, 2018; Sourakov and Shirai, 2020). Importantly, heparin likely enhances the effects of WntA in the CSS, but *fz4* mKOs only affect other heparin-sensitive patterns, implying that Fz4 is in fact unable to bind WntA. Instead, Fz4 is likely counteracting one or a combination of Wg, Wnt6 and Wnt10, which are all co-expressed in the Discalis elements and wing-peripheral region margins in larval wings (Banerjee et al., 2023; Martin and Reed, 2014). Although expression and functional assays of Wnt family members at the pupal stages will be needed to test this model, the current data suggest that sub-functionalized Fz3 and Fz4 antagonize distinct aspects of Wnt signaling in a context-dependent manner.

Conclusions

The WntA/Fz2 signaling axis has heretofore remained unstudied due to the loss of WntA in classical model systems. However, it could well prove to be evolutionarily conserved, and it will be interesting to test whether its role as a morphogen is involved in epithelial patterning elsewhere, or to identify other functions across Bilateria and Cnidaria (Hanly et al., 2021; Li et al., 2017; Schenkelaars et al., 2015). The Fz1/PCP pathway and the Wnt-antagonist role of Fz3 may both date back to pre-bilaterian ancestors (Momose and Houliston, 2007; Momose et al., 2012; Schenkelaars et al., 2015), whereas our sequence analysis suggests Fz4 only recently lost its Dsh-interacting domain during the course of insect evolution (Fig. S1B, cyan box). Overall, functional analyses of Frizzled receptors, seen under the colorful features of butterfly wings, enrich our understanding of their diverse functions in mediating cell signaling and tissue patterning.

MATERIALS AND METHODS

Butterflies

Vanessa cardui (Linnaeus 1758) were purchased from Carolina Biological Supplies, and *Junonia coenia* (Hübner 1822), originating from the laboratory of Fred Nijhout (Duke University, NC, USA) were reared on an artificial diet, in a growth chamber at 25°C, 40-60% relative humidity and under a 14:10 h light:dark cycle, following previously described procedures (Martin et al., 2020; Tendolkar et al., 2021) with the following modification: to avoid the spread of viral disease, eggs are surface decontaminated for 2 min (*V. cardui*) or 4 min (*J. coenia*) with a benzalkonium chloride 5% solution, before being dried and left to hatch on double-tape placed under the cup lids, with no more than 40 eggs per container. In these conditions, the mean pupal developmental time is 160 h for *V. cardui* and 190 h for *J. coenia.*

Agraulis incarnata (Riley 1926) is the revised species name for subspecies of (formerly named) *Agraulis vanillae* found in the USA (Núñez et al., 2022). *A. incarnata* adult butterflies were maintained in a closed enclosure situated in a rooftop greenhouse in Washington DC, with fluctuating temperatures 23-28°C and a periodic misting system for humidity. Gatorade 50% cups, *Lantana spp.* and *Buddleia spp.* provided nectaring sources. Normal feeding and sexual behavior during the day required light supplementation with six Repti-Glo 10.0 Compact Fluorescent Desert Terrarium Lamp bulbs (Exo Terra). Eggs were collected on *Passiflora biflora* or *Passiflora incarnata* and were washed for 1 min with benzalkonium chloride 5%. Larvae were reared in an incubator at 28°C, 40-60% relative humidity, and under a 14:10 h light:dark cycle. This species is prone to viral disease when crowding occurs. To remediate this, larvae were reared on artificial diet, following the *V. cardui* rearing procedure with the following modifications. Smaller batches of embryos were hatched and reared during the initial stages (n<8 individuals per cup), and larvae were moved to individual cup containers at the third larval instar. The Passionvine Butterfly artificial diet (Monarch Watch Shop), supplemented with dried *P. biflora* or *Passiflora incarnata* was used for larval feeding. Larvae required frequent movement to fresh diet cups, removal of excess silk in the fifth instar larvae and addition of a horizontal toothpick section under the cup lid to induce pre-pupal silk pad spinning.

Heliconius erato demophoon butterflies (Ménétriés 1855) and *Heliconius melpomene rosina* (Boisduval 1870) were reared at the *Heliconius* insectaries in Gamboa (Panama) and at the LMU Munich (Germany) using previously described methods (Concha et al., 2019; Rossi et al., 2020). *Danaus plexippus* (Linnaeus 1758) butterflies were reared on milkweed in greenhouse cages under standard conditions at UC San Diego (USA).

CRISPR mosaic gene knockouts

Egg microinjections were performed as previously described to deliver equimolar mixes of Cas9/sgRNA into butterfly syncytial embryos (Martin et al., 2020; Thulluru et al., 2022). In brief, sgRNAs were designed to target the transmembrane domain of the Frizzled proteins (sequences in Table S2), ordered as synthetic sgRNAs (Synthego), mixed in 1:2 mass ratio with recombinant Cas9-2xNLS (PNABio, or UC Berkeley Macrolabs-QB3) and microinjected in embryos at 1-6 h AEL. Injection conditions varied along two main parameters: time of injection after egg laying and Cas9:sgRNA duplex concentration (between 250:125 and 500:250 ng/µl). More-concentrated early injections result in large mutant clones, but can be deleterious and result in low survival. The level of mosaicism can be increased using a more-dilute mix injected at least 4 h AEL, overall resulting in higher survival, but smaller wing clones.

In situ hybridizations

Detection of mRNA expression was performed following a standard method (Martin and Reed, 2014), with minor modifications for early pupal wings. Pupal wings at 13-17% development tissues were dissected in ice-cold 1× phosphate-buffered saline (PBS). A scalpel or straight Vannas Spring Scissors (8 cm/2.5 mm tip) were used to cut the contour of forewing, which was then detached from the pupal case by first grabbing the base then pulling the wing carefully towards the distal edge; forceps were used to remove part of the peripodial membranes while keeping for forewings and hindwings embedded at their edges. Forewings were placed back to the cuticle and transferred to fixative (1×PBS, 10 mM EGTA and 9.25% formaldehyde) for 30-40 min at room temperature, together with the entire pupal case with the hindwings attached. After fixing, wings were washed with ice-cold PBT (1×PBS and 0.1% Tween20) twice, while still embedded in their cuticle or pupal case, which was then removed with fine forceps. Subsequent PBT washes and the rest of the published protocol were carried out with two pupal wings per tube. For the final development of stains, wings were incubated in BM Purple (Roche Applied Science) for 10-15 h at room temperature. Riboprobes for *WntA* and *wg* have been previously described (Martin and Reed, 2014). Riboprobes for the four *frizzled* genes were PCR amplified from *V. cardui* cDNA (Table S4), transcribed with a Roche T7 DIG RNA labeling kit, purified with Ambion MEGAClear columns and stored at −80°C. Images were taken using a Nikon D5300 camera mounted to a Nikon SMZ800N trinocular dissecting microscope, equipped with a P-Plan Apo 1×/WF 0.105 NA 70 mm objective and a Nikon C-DS stand for diascopic mirror illumination.

siRNA electroporations

Dicer-substrate siRNAs (DsiRNAs) were designed against nymphalid *fz1*- and *fz2*-coding sequences (Table S5) using both the online IDT siRNA designer tool and the siRNA iScore Designer web services (Ichihara et al., 2007), ordered at the 2 nmol or 10 nmol scales as Custom DsiRNAs with standard purification (IDT DNA Technologies), resuspended at 70-100 µM in 1× *Bombyx* injection buffer (pH 7.2; 0.5 mM NaH_2PO_4, 0.5 mM Na_2HPO_4 and 5 mM KCl), and stored as frozen aliquots at −80°C until use. Electroporations were conducted within 30 min of the onset of pupation using a BTX ECM 830 electroporator with gold electrodes (Harvard Apparatus, Genetrodes bent gold tip, 5 mm). Electroporation procedures followed a previously described procedure (Fujiwara and Nishikawa, 2016). In brief, pupal forewings were lifted over a thin pad of 1% agarose prepared in 10×PBS, injected in their ventral surface with 1-4 µl of annealed siRNA mix (distal to the discal vein) and covered with a 20-30 µl droplet of 1×PBS.

Development (2023) 150, dev201868. doi:10.1242/dev.201868

The positive electrode was placed in contact with the droplet, taking great care to not touch the wing epithelium (see below), while the negative electrode was in contact with the agarose pad on the dorsal side of the wing, before electroporation with five square pulses of 280 ms at 9-15 V, separated by 100 ms intervals. The PBS droplet was removed before reinsertion of the forewing into its pupal case. Pupae were sprayed with water every 2 days before emergence to avoid desiccation. In order to control for potential artifacts of the procedure, sham controls using GFP siRNA injections and injection dye were run. GFP siRNAs were injected into forewings or hindwings and electroporated with five square pulses of 280 ms at 8-15 V, separated by 100 ms intervals. Similarly, Phenol Red (2-4 µl) was injected at a concentration of 0.05% to monitor injection spread across the forewing. In the red dye injection experiments, to test for potential effects of excessive current, the positive electrode was directly placed in contact with the wing tissue within a PBS droplet, before electroporation using 6 V to 9 V at 280 ms, 5 pulses with 100 ms interval each.

Wing vein imaging

Wings were de-scaled by washing in 90% ethanol for ∼3 min, then switching to 10% Clorox bleach for 3 min, and repeating until the scales and pigments were removed from the wings. Washed wings were then imaged on a Keyence VHX-5000 microscope mounted with a VH-Z00 T lens.

In vivo sgRNA validation by genotyping

Sanger sequencing of G_0 crispants was performed to verify the induction of indels at the predicted cut sites for several sgRNAs (Fig. S21). Thoracic muscle from adult *fz2* crispants was amplified by PCR, followed by clean-up and sequencing (*V. cardui*), or isolated in single bacterial colonies by TA cloning before sequencing (*D. plexippus*). For *fz1*, *fz2* and *fz4* (*V. cardui*), CRISPR injections were performed 30-45 min AEL to limit mosaicism, targets from single crispant embryos (24 h or 48 h AEL) were amplified using Phire Tissue Direct PCR Master Mix (Invitrogen, diluted protocol), and 45 µL reactions were purified using the PureLink PCR purification kit (Invitrogen) and sequenced. *V. cardui fz1* and *fz3* crispant chromatograms contained multiple indel alleles and were analyzed using TIDE analysis (Brinkman et al., 2014). Primer sequences are provided in Table S3.

Acknowledgements

We thank Rachel Canalichio and the staff of the Wilbur V. Harlan Greenhouse at the GWU for butterfly rearing and host plant resources; Bob Reed, Brian Counterman and Donya Shodja for stimulating discussions and comments on the manuscript; Chip Taylor and Ann Ryan for providing Passionvine Butterfly artificial diet; and Richard Merrill for facilitating *H. melpomene* experiments.

Competing interests

The authors declare no competing or financial interests.

Author contributions

Conceptualization: J.J.H., L.S.L., A.M.; Investigation: J.J.H., L.S.L., A.M.-V., T.S.R.-M., L.L., A.T., C.R.D., N.L., E.A.E., O.B.W.H.C., N.D., J.J.H.-P., C.M., J.A.A., M.R., M.W.P., A.M.; Writing - original draft: J.J.H., L.S.L., A.M.; Visualization: J.J.H., L.S.L., A.M.; Supervision: J.J.H., R.P., W.O.M., M.W.P., A.M.; Funding acquisition: J.J.H., R.P., W.M., A.M.

Funding

This work was funded by the National Science Foundation (IOS-1656553 and IOS-2110534 to A.M.; EPSCoR 1736026 and IOS 1656389 to R.P.), by a Smithsonian Biodiversity Genomics Postdoctoral Fellowship (to J.J.H.), by Harlan Summer (to L.S.L., A.T., E.A.E. and O.B.W.H.C) and Luther Rice (to J.J.H.-P.) fellowships at The George Washington University, by a National Science Foundation PRFB fellowship (to A.M.V.) and by the Deutsche Forschungsgemeinschaft (ME4845/1-1). Open Access funding provided by The George Washington University. Deposited in PMC for immediate release.

Data availability

All relevant data can be found within the article and its supplementary information.

References

Adler, P. N. (2012). The frizzled/stan pathway and planar cell polarity in the Drosophila wing. *Curr. Top. Dev. Biol.* **101**, 1-31. doi:10.1016/B978-0-12-394592-1.00001-6

Agrawal, T. and Hasan, G. (2015). Maturation of a central brain flight circuit in Drosophila requires Fz2/Ca2+ signaling. *Elife* **4**, e07046. doi:10.7554/eLife.07046

Alvarez-Rodrigo, I., Willnow, D. and Vincent, J.-P. (2023). Chapter One - The logistics of Wnt production and delivery. In *Current Topics in Developmental Biology* (ed. T. P. Yamaguchi and K. Willert), pp. 1-60. Academic Press.

Banerjee, T. D. and Monteiro, A. (2020). Molecular mechanisms underlying simplification of venation patterns in holometabolous insects. *Development* **147**, dev196394. doi:10.1242/dev.196394

Banerjee, T. D., Murugesan, S. N., Connahs, H. and Monteiro, A. (2023). Spatial and temporal regulation of Wnt signaling pathway members in the development of butterfly wing patterns. *Sci. Adv.* **9**, eadg3877. doi:10.1126/sciadv.adg3877

Beermann, A., Prühs, R., Lutz, R. and Schröder, R. (2011). A context-dependent combination of Wnt receptors controls axis elongation and leg development in a short germ insect. *Development* **138**, 2793-2805. doi:10.1242/dev.063644

Bhanot, P., Fish, M., Jemison, J. A., Nusse, R., Nathans, J. and Cadigan, K. M. (1999). Frizzled and Dfrizzled-2 function as redundant receptors for Wingless during Drosophila embryonic development. *Development* **126**, 4175-4186. doi:10.1242/dev.126.18.4175

Bolognesi, R., Farzana, L., Fischer, T. D. and Brown, S. J. (2008). Multiple Wnt genes are required for segmentation in the short-germ embryo of Tribolium castaneum. *Curr. Biol.* **18**, 1624-1629. doi:10.1016/j.cub.2008.09.057

Brennan, K., Klein, T., Wilder, E. and Arias, A. M. (1999). Wingless modulates the effects of dominant negative notch molecules in the developing wing of Drosophila. *Dev. Biol.* **216**, 210-229. doi:10.1006/dbio.1999.9502

Brinkman, E. K., Chen, T., Amendola, M. and Van Steensel, B. (2014). Easy quantitative assessment of genome editing by sequence trace decomposition. *Nucleic Acids Res.* **42**, e168-e168. doi:10.1093/nar/gku936

Brunetti, C. R., Selegue, J. E., Monteiro, A., French, V., Brakefield, P. M. and Carroll, S. B. (2001). The generation and diversification of butterfly eyespot color patterns. *Curr. Biol.* **11**, 1578-1585. doi:10.1016/S0960-9822(01)00502-4

Buceta, J., Herranz, H., Canela-Xandri, O., Reigada, R., Sagués, F. and Milán, M. (2007). Robustness and stability of the gene regulatory network involved in DV boundary formation in the Drosophila wing. *PLoS One* **2**, e602. doi:10.1371/journal.pone.0000602

Butler, M. T. and Wallingford, J. B. (2017). Planar cell polarity in development and disease. *Nat. Rev. Mol. Cell Biol.* **18**, 375-388. doi:10.1038/nrm.2017.11

Cadigan, K. M., Fish, M. P., Rulifson, E. J. and Nusse, R. (1998). Wingless repression of Drosophila frizzled 2 expression shapes the Wingless morphogen gradient in the wing. *Cell* **93**, 767-777. doi:10.1016/S0092-8674(00)81438-5

Chaudhary, V., Hingole, S., Frei, J., Port, F., Strutt, D. and Boutros, M. (2019). Robust Wnt signaling is maintained by a Wg protein gradient and Fz2 receptor activity in the developing Drosophila wing. *Development* **146**, dev174789. doi:10.1242/dev.174789

Chen, C. M. and Struhl, G. (1999). Wingless transduction by the Frizzled and Frizzled2 proteins of Drosophila. *Development* **126**, 5441-5452. doi:10.1242/dev.126.23.5441

Cohen, E. D., Mariol, M.-C., Wallace, R. M., Weyers, J., Kamberov, Y. G., Pradel, J. and Wilder, E. L. (2002). DWnt4 regulates cell movement and focal adhesion kinase during Drosophila ovarian morphogenesis. *Dev. Cell* **2**, 437-448. doi:10.1016/S1534-5807(02)00142-9

Concha, C., Wallbank, R. W. R., Hanly, J. J., Fenner, J., Livraghi, L., Rivera, E. S., Paulo, D. F., Arias, C., Vargas, M., Sanjeev, M. et al. (2019). Interplay between developmental flexibility and determinism in the evolution of mimetic heliconius wing patterns. *Curr. Biol.* **29**, 3996-4009.e4. doi:10.1016/j.cub.2019.10.010

Connahs, H., Tlili, S., Van Creij, J., Loo, T. Y., Banerjee, T. D., Saunders, T. E. and Monteiro, A. (2019). Activation of butterfly eyespots by Distal-less is consistent with a reaction-diffusion process. *Development* **146**, dev169367. doi:10.1242/dev.169367

Darras, S., Fritzenwanker, J. H., Uhlinger, K. R., Farrelly, E., Pani, A. M., Hurley, I. A., Norris, R. P., Osovitz, M., Terasaki, M. and Wu, M. et al. (2018). Anteroposterior axis patterning by early canonical Wnt signaling during hemichordate development. *PLoS Biol.* **16**, e2003698. doi:10.1371/journal.pbio.2003698

Day, C. R., Hanly, J. J., Ren, A. and Martin, A. (2019). Sub-micrometer insights into the cytoskeletal dynamics and ultrastructural diversity of butterfly wing scales. *Dev. Dyn.* **248**, 657-670. doi:10.1002/dvdy.63

Dinwiddie, A., Null, R., Pizzano, M., Chuong, L., Krup, A. L., Tan, H. E. and Patel, N. H. (2014). Dynamics of F-actin prefigure the structure of butterfly wing scales. *Dev. Biol.* **392**, 404-418. doi:10.1016/j.ydbio.2014.06.005

Ewen-Campen, B., Comyn, T., Vogt, E. and Perrimon, N. (2020). No evidence that Wnt ligands are required for planar cell polarity in Drosophila. *Cell Rep. Reports* **32**, 108121. doi:10.1016/j.celrep.2020.108121

Fenner, J., Benson, C., Rodriguez-Caro, L., Ren, A., Papa, R., Martin, A., Hoffmann, F., Range, R. and Counterman, B. A. (2020). Wnt genes in wing pattern development of Coliadinae butterflies. *Front. Ecol. Evol.* **8**, 00197. doi:10.3389/fevo.2020.00197

Fujiwara, H. and Nishikawa, H. (2016). Functional analysis of genes involved in color pattern formation in Lepidoptera. *Curr. Opin. Insect Sci.* **17**, 16-23. doi:10.1016/j.cois.2016.05.015
Gallant, J. R., Imhoff, V. E., Martin, A., Savage, W. K., Chamberlain, N. L., Pote, B. L., Peterson, C., Smith, G. E., Evans, B., Reed, R. D. et al. (2014). Ancient homology underlies adaptive mimetic diversity across butterflies. *Nat. Commun.* **5**, 4817. doi:10.1038/ncomms5817
Gao, C. and Chen, Y.-G. (2010). Dishevelled: the hub of Wnt signaling. *Cell. Signal.* **22**, 717-727. doi:10.1016/j.cellsig.2009.11.021
Gieseler, K., Wilder, E., Mariol, M.-C., Buratovitch, M., Bérenger, H., Graba, Y. and Pradel, J. (2001). DWnt4 and wingless elicit similar cellular responses during imaginal development. *Dev. Biol.* **232**, 339-350. doi:10.1006/dbio.2001.0184
Hanly, J. J., Wallbank, R. W., Mcmillan, W. O. and Jiggins, C. D. (2019). Conservation and flexibility in the gene regulatory landscape of heliconiine butterfly wings. *Evodevo* **10**, 15. doi:10.1186/s13227-019-0127-4
Hanly, J. J., Robertson, E. C. N., Corning, O. B. W. H. and Martin, A. (2021). Porcupine/Wntless-dependent trafficking of the conserved WntA ligand in butterflies. *J. Exp. Zoolo. Part B: Mol. Dev. Evol.* **336**, 470-481. doi:10.1002/jez.b.23046
Hoppler, S. P. and Moon, R. T. (2014). *Wnt Signaling in Development and Disease: Molecular Mechanisms and Biological Functions*. John Wiley & Sons.
Ichihara, M., Murakumo, Y., Masuda, A., Matsuura, T., Asai, N., Jijiwa, M., Ishida, M., Shinmi, J., Yatsuya, H. and Qiao, S. et al. (2007). Thermodynamic instability of siRNA duplex is a prerequisite for dependable prediction of siRNA activities. *Nucleic Acids Res.* **35**, e123. doi:10.1093/nar/gkm699
Iwata, M. and Otaki, J. M. (2019). Insights into eyespot color-pattern formation mechanisms from color gradients, boundary scales, and rudimentary eyespots in butterfly wings. *J. Insect Physiol.* **114**, 68-82. doi:10.1016/j.jinsphys.2019.02.009
Janssen, R., Schönauer, A., Weber, M., Turetzek, N., Hogvall, M., Goss, G. E., Patel, N. H., Mcgregor, A. P. and Hilbrant, M. (2015). The evolution and expression of panarthropod frizzled genes. *Front. Ecol. Evol.* **3**, 96. doi:10.3389/fevo.2015.00096
Jiggins, C. D., Wallbank, R. W. and Hanly, J. J. (2017). Waiting in the wings: what can we learn about gene co-option from the diversification of butterfly wing patterns? *Philos. Trans. R. Soc. B: Biol. Sci.* **372**, 20150485. doi:10.1098/rstb.2015.0485
Joyce, J. S., Maugarny-Calès, A., Pelletier, S., Alexandre, C., Bellaiche, Y., Vincent, J.-P. and Mcgough, I. J. (2020). Frizzled-dependent planar cell polarity without secreted Wnt ligands. *Dev. Cell* **54**, 583-592.e5. doi:10.1016/j.devcel.2020.08.004
Kraus, Y., Aman, A., Technau, U. and Genikhovich, G. (2016). Pre-bilaterian origin of the blastoporal axial organizer. *Nat. Commun.* **7**, 11694. doi:10.1038/ncomms11694
Lander, A. D. (2007). Morpheus unbound: reimagining the morphogen gradient. *Cell* **128**, 245-256. doi:10.1016/j.cell.2007.01.004
Lawrence, P. A. and Casal, J. (2018). Planar cell polarity: two genetic systems use one mechanism to read gradients. *Development* **145**, dev168229. doi:10.1242/dev.168229
Li, X., Sun, L., Yang, H., Zhang, L., Miao, T., Xing, L. and Huo, D. (2017). Identification and expression characterization of WntA during intestinal regeneration in the sea cucumber Apostichopus japonicus. *Comp. Biochem. Physiol. B: Biochem. Mol. Biol.* **210**, 55-63. doi:10.1016/j.cbpb.2017.06.005
Linnemannstöns, K., Ripp, C., Honemann-Capito, M., Brechtel-Curth, K., Hedderich, M. and Wodarz, A. (2014). The PTK7-related transmembrane proteins off-track and off-track 2 are co-receptors for Drosophila Wnt2 required for male fertility. *PLoS Genet.* **10**, e1004443. doi:10.1371/journal.pgen.1004443
Livraghi, L., Martin, A., Gibbs, M., Braak, N., Arif, S. and Breuker, C. J. (2018). CRISPR/Cas9 as the key to unlocking the secrets of butterfly wing pattern development and its evolution. *Adv. Insect Physiol.* **54**, 85-115. doi:10.1016/bs.aiip.2017.11.001
López-Varea, A., Vega-Cuesta, P., Ruiz-Gómez, A., Ostalé, C. M., Molnar, C., Hevia, C. F., Martín, M., Organista, M. F., De Celis, J. and Culí, J. et al. (2021a). Genome-wide phenotypic RNAi screen in the Drosophila wing: phenotypic description of functional classes. *G3* **11**, jkab349. doi:10.1093/g3journal/jkab349
López-Varea, A., Ostalé, C. M., Vega-Cuesta, P., Ruiz-Gómez, A., Organista, M. F., Martín, M., Hevia, C. F., Molnar, C., De Celis, J. and Culi, J. et al. (2021b). Genome-wide phenotypic RNAi screen in the Drosophila wing: global parameters. *G3* **11**, jkab351. doi:10.1093/g3journal/jkab351
Lunde, K., Trimble, J. L., Guichard, A., Guss, K. A., Nauber, U. and Bier, E. (2003). Activation of the knirps locus links patterning to morphogenesis of the second wing vein in Drosophila. *Development* **130**, 235-248. doi:10.1242/dev.00207
Macdonald, W. P., Martin, A. and Reed, R. D. (2010). Butterfly wings shaped by a molecular cookie cutter: evolutionary radiation of lepidopteran wing shapes associated with a derived Cut/wingless wing margin boundary system. *Evol. Dev.* **12**, 296-304. doi:10.1111/j.1525-142X.2010.00415.x
Martin, A. and Courtier-Orgogozo, V. (2017). Morphological evolution repeatedly caused by mutations in signaling ligand genes. In *Diversity and Evolution of Butterfly Wing Patterns - an Integrative Approach* (T. Sekimura and H. F. Nijhout, eds), Chapter 4. Springer. doi:10.1007/978-981-10-4956-9_4
Martin, A. and Reed, R. D. (2010). Wingless and aristaless2 define a developmental ground plan for moth and butterfly wing pattern evolution. *Mol. Biol. Evol.* **27**, 2864-2878. doi:10.1093/molbev/msq173
Martin, A. and Reed, R. D. (2014). Wnt signaling underlies evolution and development of the butterfly wing pattern symmetry systems. *Dev. Biol.* **395**, 367-378. doi:10.1016/j.ydbio.2014.08.031
Martin, A., Papa, R., Nadeau, N. J., Hill, R. I., Counterman, B. A., Halder, G., Jiggins, C. D., Kronforst, M. R., Long, A. D., Mcmillan, W. O. et al. (2012). Diversification of complex butterfly wing patterns by repeated regulatory evolution of a Wnt ligand. *Proc. Natl. Acad. Sci. USA* **109**, 12632-12637. doi:10.1073/pnas.1204800109
Martin, A., Wolcott, N. S. and O'connell, L. A. (2020). Bringing immersive science to undergraduate laboratory courses using CRISPR gene knockouts in frogs and butterflies. *J. Exp. Biol.* **223**, jeb208793. doi:10.1242/jeb.208793
Mathew, D., Ataman, B., Chen, J., Zhang, Y., Cumberledge, S. and Budnik, V. (2005). Wingless signaling at synapses is through cleavage and nuclear import of receptor DFrizzled2. *Science* **310**, 1344-1347. doi:10.1126/science.1117051
Mazo-Vargas, A., Concha, C., Livraghi, L., Massardo, D., Wallbank, R. W., Zhang, L., Papador, J. D., Martinez-Najera, D., Jiggins, C. D. and Kronforst, M. R. (2017).). Macroevolutionary shifts of WntA function potentiate butterfly wing-pattern diversity. *Proc. Natl. Acad. Sci. USA* **114**, 10701-10706. doi:10.1073/pnas.1708149114
Mazo-Vargas, A., Langmüller, A. M., Wilder, A., Van Der Burg, K. R., Lewis, J. J., Messer, P. W., Zhang, L., Martin, A. and Reed, R. D. (2022). Deep cis-regulatory homology of the butterfly wing pattern ground plan. *Science* **378**, 304-308. doi:10.1126/science.abi9407
Mckenna, K. Z., Kudla, A. M. and Nijhout, H. F. (2020). Anterior–posterior patterning in lepidopteran wings. *Front. Ecol. Evol.* **8**, 146. doi:10.3389/fevo.2020.00146
Mcmillan, W. O., Livraghi, L., Concha, C. and Hanly, J. J. (2020). From patterning genes to process: unraveling the gene regulatory networks that pattern Heliconius wings. *Front. Ecol. Evol.* **8**, 221. doi:10.3389/fevo.2020.00221
Mehta, S., Hingole, S. and Chaudhary, V. (2021). The emerging mechanisms of Wnt secretion and signaling in development. *Front. Cell Dev. Biol.* **9**, 714746. doi:10.3389/fcell.2021.714746
Mieszczanek, J., Strutt, H., Rutherford, T. J., Strutt, D., Bienz, M. and Gammons, M. V. (2022). Selective function of the PDZ domain of Dishevelled in noncanonical Wnt signalling. *J. Cell Sci.* **135**, jcs259547. doi:10.1242/jcs.259547
Moline, M. M., Dierick, H. A., Southern, C. and Bejsovec, A. (2000). Non-equivalent roles of Drosophila Frizzled and Dfrizzled2 in embryonic wingless signal transduction. *Curr. Biol.* **10**, 1127-1130. doi:10.1016/S0960-9822(00)00697-7
Momose, T. and Houliston, E. (2007). Two oppositely localised frizzled RNAs as axis determinants in a cnidarian embryo. *PLoS Biol.* **5**, e70. doi:10.1371/journal.pbio.0050070
Momose, T., Kraus, Y. and Houliston, E. (2012). A conserved function for Strabismus in establishing planar cell polarity in the ciliated ectoderm during cnidarian larval development. *Development* **139**, 4374-4382. doi:10.1242/dev.084251
Monteiro, A. (2015). Origin, development, and evolution of butterfly eyespots. *Annu. Rev. Entomol.* **60**, 253-271. doi:10.1146/annurev-ento-010814-020942
Morris, J., Hanly, J. J., Martin, S. H., Van Belleghem, S. M., Salazar, C., Jiggins, C. D. and Dasmahapatra, K. K. (2020). Deep convergence, shared ancestry, and evolutionary novelty in the genetic architecture of Heliconius mimicry. *Genetics* **216**, 765-780. doi:10.1534/genetics.120.303611
Nijhout, H. F. (1991). *The Development and Evolution of Butterfly Wing Patterns*. Washington: Smithsonian Institution Press.
Nijhout, H. F. (2017). The common developmental origin of eyespots and parafocal elements and a new model mechanism for color pattern formation. In *Diversity and Evolution of Butterfly Wing Patterns: An Integrative Approach* (T. Sekimura and H. F. Nijhout, eds), pp. 3-19. Springer
Nijhout, H. F. and Wray, G. A. (1988). Homologies in the color patterns of the genus heliconius (Lepidoptera, Nymphalidae). *Biol. J. Linn. Soc.* **33**, 345-365. doi:10.1111/j.1095-8312.1988.tb00449.x
Nile, A. H. and Hannoush, R. N. (2019). Fatty acid recognition in the Frizzled receptor family. *J. Biol. Chem.* **294**, 726-736. doi:10.1074/jbc.REV118.005205
Núñez, R., Willmott, K. R., Álvarez, Y., Genaro, J. A., Pérez-Asso, A. R., Quejereta, M., Turner, T., Miller, J. Y., Brévignon, C. and Lamas, G. et al. (2022). Integrative taxonomy clarifies species limits in the hitherto monotypic passion-vine butterfly genera Agraulis and Dryas (Lepidoptera, Nymphalidae, Heliconiinae). *Syst. Entomol.* **47**, 152-178. doi:10.1111/syen.12523
Otaki, J. M. (2012). Color pattern analysis of nymphalid butterfly wings: revision of the nymphalid groundplan. *Zoolog. Sci.* **29**, 568-576. doi:10.2108/zsj.29.568
Peradziryi, H., Kaplan, N. A., Podleschny, M., Liu, X., Wehner, P., Borchers, A. and Tolwinski, N. S. (2011). PTK7/Otk interacts with Wnts and inhibits canonical Wnt signalling. *EMBO J.* **30**, 3729-3740. doi:10.1038/emboj.2011.236
Povelones, M. and Nusse, R. (2005). The role of the cysteine-rich domain of Frizzled in Wingless-Armadillo signaling. *EMBO J.* **24**, 3493-3503. doi:10.1038/sj.emboj.7600817

Reed, R. D. and Gilbert, L. E. (2004). Wing venation and Distal-less expression in Heliconius butterfly wing pattern development. *Dev. Genes Evol.* **214**, 628-634. doi:10.1007/s00427-004-0439-8
Reed, R. D., Chen, P.-H. and Nijhout, F. H. (2007). Cryptic variation in butterfly eyespot development: the importance of sample size in gene expression studies. *Evol. Dev.* **9**, 2-9. doi:10.1111/j.1525-142X.2006.00133.x
Restrepo, L. J., Depew, A. T., Moese, E. R., Tymanskyj, S. R., Parisi, M. J., Aimino, M. A., Duhart, J. C., Fei, H. and Mosca, T. J. (2022). γ-secretase promotes Drosophila postsynaptic development through the cleavage of a Wnt receptor. *Dev. Cell* **57**, 1643-1660.e7. doi:10.1016/j.devcel.2022.05.006
Ripp, C., Loth, J., Petrova, I., Linnemannstöns, K., Ulepic, M., Fradkin, L., Noordermeer, J. and Wodarz, A. (2018). Drosophila Ror is a nervous system-specific co-receptor for Wnt ligands. *Biol. Open* **7**, bio033001. doi:10.1242/bio.033001
Rossi, M., Hausmann, A. E., Thurman, T. J., Montgomery, S. H., Papa, R., Jiggins, C. D., Mcmillan, W. O. and Merrill, R. M. (2020). Visual mate preference evolution during butterfly speciation is linked to neural processing genes. *Nat. Commun.* **11**, 4763. doi:10.1038/s41467-020-18609-z
Ruttenberg, D. M., VanKuren, N. W., Nallu, S., Yen, S.-H., Peggie, D., Lohman, D. J. and Kronforst, M. R. (2021). The evolution and genetics of sexually dimorphic 'dual' mimicry in the butterfly Elymnias hypermnestra. *Proc. R. Soc. B* **288**, 20202192. doi:10.1098/rspb.2020.2192
Sagner, A. and Briscoe, J. (2017). Morphogen interpretation: concentration, time, competence, and signaling dynamics. *Wiley Interdiscip. Rev. Dev. Biol.* **6**, e271. doi:10.1002/wdev.271
Sato, A., Kojima, T., Ui-Tei, K., Miyata, Y. and Saigo, K. (1999). Dfrizzled-3, a new Drosophila Wnt receptor, acting as an attenuator of Wingless signaling in wingless hypomorphic mutants. *Development* **126**, 4421-4430. doi:10.1242/dev.126.20.4421
Schenkelaars, Q., Fierro-Constain, L., Renard, E., Hill, A. L. and Borchiellini, C. (2015). Insights into Frizzled evolution and new perspectives. *Evol. Dev.* **17**, 160-169. doi:10.1111/ede.12115
Schilling, S., Steiner, S., Zimmerli, D. and Basler, K. (2014). A regulatory receptor network directs the range and output of the Wingless signal. *Development* **141**, 2483-2493. doi:10.1242/dev.108662
Serfas, M. S. and Carroll, S. B. (2005). Pharmacologic approaches to butterfly wing patterning: sulfated polysaccharides mimic or antagonize cold shock and alter the interpretation of gradients of positional information. *Dev. Biol.* **287**, 416-424. doi:10.1016/j.ydbio.2005.09.014
Shi, F., Mendrola, J. M., Sheetz, J. B., Wu, N., Sommer, A., Speer, K. F., Noordermeer, J. N., Kan, Z.-Y., Perry, K. and Englander, S. W. et al. (2021). ROR and RYK extracellular region structures suggest that receptor tyrosine kinases have distinct WNT-recognition modes. *Cell Rep.* **37**, 109834. doi:10.1016/j.celrep.2021.109834
Somorjai, I. M., Martí-Solans, J., Diaz-Gracia, M., Nishida, H., Imai, K. S., Escrivà, H., Cañestro, C. and Albalat, R. (2018). Wnt evolution and function shuffling in liberal and conservative chordate genomes. *Genome Biol.* **19**, 98. doi:10.1186/s13059-018-1468-3
Sourakov, A. (2018). Emperors, admirals and giants, zebras, tigers and woolly bears: casting a broader net in exploring heparin effects on Lepidoptera wing patterns. *F1000Res.* **7**, 1842. doi:10.12688/f1000research.16926.3
Sourakov, A. and Shirai, L. T. (2020). Pharmacological and surgical experiments on wing pattern development of Lepidoptera, with a focus on the eyespots of saturniid moths. *Trop. Lepid. Res.* **30**, 4-19.
Strutt, D., Madder, D., Chaudhary, V. and Artymiuk, P. J. (2012). Structure–function dissection of the Frizzled receptor in Drosophila melanogaster suggests different mechanisms of action in planar polarity and canonical Wnt signaling. *Genetics* **192**, 1295-1313. doi:10.1534/genetics.112.144592
Swarup, S. and Verheyen, E. M. (2012). Wnt/Wingless signaling in Drosophila. *Cold Spring Harbor Perspect. Biol.* **4**, a007930. doi:10.1101/cshperspect.a007930
Taira, W., Kinjo, S. and Otaki, J. M. (2015). The marginal band system in nymphalid butterfly wings. *Zoolog. Sci.* **32**, 38-46. doi:10.2108/zs140058
Tauriello, D. V., Jordens, I., Kirchner, K., Slootstra, J. W., Kruitwagen, T., Bouwman, B. A., Noutsou, M., Rüdiger, S. G., Schwamborn, K. and Schambony, A. et al. (2012). Wnt/β-catenin signaling requires interaction of the Dishevelled DEP domain and C terminus with a discontinuous motif in Frizzled. *Proc. Natl. Acad. Sci. USA* **109**, E812-E820. doi:10.1073/pnas.1114802109
Tendolkar, A., Pomerantz, A. F., Heryanto, C., Shirk, P. D., Patel, N. H. and Martin, A. (2021). Ultrabithorax is a micromanager of hindwing identity in butterflies and moths. *Front. Ecol. Evol.* **9**, 643661. doi:10.3389/fevo.2021.643661
Thulluru, A., Saad, L., Nagah Abdou, Y., Martin, A. and Kee, H. L. (2022). CRISPR in butterflies: an undergraduate lab experience to inactivate wing patterning genes during development. *Biochem. Mol. Biol. Educ.* **50**, 605-619. doi:10.1002/bmb.21669
Tunström, K., Woronik, A., Hanly, J. J., Rastas, P., Chichvarkhin, A., Warren, A. D., Kawahara, A. Y., Schoville, S. D., Ficarrotta, V. and Porter, A. H. (2023). Evidence for a single, ancient origin of a genus-wide alternative life history strategy. *Sci. Adv.* **9**, eabq3713. doi:10.1126/sciadv.abq3713
Van Belleghem, S. M., Rastas, P., Papanicolaou, A., Martin, S. H., Arias, C. F., Supple, M. A., Hanly, J. J., Mallet, J., Lewis, J. J., Hines, H. M. et al. (2017). Complex modular architecture around a simple toolkit of wing pattern genes. *Nat. Ecol. Evol.* **1**, 52. doi:10.1038/s41559-016-0052
Van Belleghem, S. M., Alicea Roman, P. A., Carbia Gutierrez, H., Counterman, B. A. and Papa, R. (2020). Perfect mimicry between Heliconius butterflies is constrained by genetics and development. *Proc. R. Soc. B* **287**, 20201267. doi:10.1098/rspb.2020.1267
Van Belleghem, S. M., Lewis, J. J., Rivera, E. S. and Papa, R. (2021). Heliconius butterflies: a window into the evolution and development of diversity. *Curr. Opin. Genet. Dev.* **69**, 72-81. doi:10.1016/j.gde.2021.01.010
VanKuren, N. W., Doellman, M. M., Sheikh, S. I., Palmer Droguett, D. H., Massardo, D. and Kronforst, M. R. (2023). Acute and long-term consequences of co-opted doublesex on the development of mimetic butterfly color patterns. *Mol. Biol. Evol.* **40**, msad196. doi:10.1093/molbev/msad196
Westerman, E. L., VanKuren, N. W., Massardo, D., Tenger-Trolander, A., Zhang, W., Hill, R. I., Perry, M., Bayala, E., Barr, K. and Chamberlain, N. et al. (2018). Aristaless controls butterfly wing color variation used in mimicry and mate choice. *Curr. Biol.* **28**, 3469-3474. doi:10.1016/j.cub.2018.08.051
Yang, Y. and Mlodzik, M. (2015). Wnt-Frizzled/planar cell polarity signaling: cellular orientation by facing the wind (Wnt). *Annu. Rev. Cell Dev. Biol.* **31**, 623-646. doi:10.1146/annurev-cellbio-100814-125315
Zeng, Y. A., Rahnama, M., Wang, S., Lee, W. and Verheyen, E. M. (2008). Inhibition of Drosophila Wg signaling involves competition between Mad and Armadillo/β-Catenin for dTcf binding. *PLoS One* **3**, e3893. doi:10.1371/journal.pone.0003893
Zhang, J. and Carthew, R. W. (1998). Interactions between Wingless and DFz2 during Drosophila wing development. *Development* **125**, 3075-3085. doi:10.1242/dev.125.16.3075
Zhang, L., Mazo-Vargas, A. and Reed, R. D. (2017a). Single master regulatory gene coordinates the evolution and development of butterfly color and iridescence. *Proc. Natl. Acad. Sci. USA* **114**, 10707-10712. doi:10.1073/pnas.1709058114
Zhang, L., Martin, A., Perry, M. W., Van Der Burg, K. R. L., Matsuoka, Y., Monteiro, A. and Reed, R. D. (2017b). Genetic basis of melanin pigmentation in butterfly wings. *Genetics* **205**, 1537-1550. doi:10.1534/genetics.116.196451